communications materials

Article

https://doi.org/10.1038/s43246-024-00504-5

Fabrication of stable monolayer liquid marbles with reduced particle coverage and locomotion on hydrophilic surface

Jing Jin [1,4] ✉, Zheng Huang[1,2,4], Yuanhao Xie[1,2], Zheng Shen[2], Bo Liu[3] & Huaying Chen [1] ✉

Liquid marbles are non-wetting, particle-covered microdroplets with a core-shell structure that are used in sample transport, material synthesis, and real-time sensing. Optimizing the distribution of shell particles remains a challenge, due to a tendency for aggregation *via* spontaneous assembly, which often leads to multilayered structures. Here, we outline a simple method for fabricating water-filled, monolayer liquid marbles with adjustable particle coverage rates, greatly reducing particle consumption. The soft liquid marbles are enclosed by a small quantity of modified polystyrene microspheres and display good atmospheric stability. The rolling behavior of flexible liquid marbles with wide coverage rates is then characterized. Contrary to common perception, the marbles with transparent openings exhibit high maneuverability on hydrophilic surfaces, and also excel in fusion, reaction and surface cleaning, with an elongated operational duration and a wide visualization range. The study provides new insights into the implementation of liquid marble-based miniaturized platforms.

Liquids play a ubiquitous role in life and form a sturdy foundation for our evolving world. Even a minuscule volume of liquid, such as a droplet, can contain an abundance of physical or biochemical information[1–4]. Therefore, the precise handling of liquid, especially regarding safety, is a perennial topic, where a non-wetting surface for droplet manipulation is highly valued[5–7]. Inspired by the lotus effect in nature, superhydrophobic surfaces created by chemical modification or structural patterning have been extensively researched for the smooth transport of droplets[8–10]. Additionally, liquid marbles (LMs), artificial non-wetting droplet microsystems, have also emerged as an effective and straightforward solution for manipulating droplets, as they function by wrapping bare droplets in a stretchable particle shell[11,12]. Similar to raindrops falling on dust and alkaline water pouring on wheat flour, LMs can be readily formed by rolling bare droplets on a solid particle bed, regardless of their hydrophobicity. Compared to the Pickering emulsions developed in the 20th century, LMs with flexible material combinations are now not only used for common liquid handling tasks but also frequently chosen as independent miniaturized chambers[13,14]. These LMs offer a few advantages over conventional droplet systems, including but not limited to inherent anti-wetting property, good mobility, low evaporation, three-dimensional (3D) interior structure and physically zero cross-contamination[15,16].

As a typical soft matter, LMs could serve as efficient platforms for digital microfluidics, soft robotics, biochemical analysis, cellular science, and also information transfer[13]. The key to the widespread use of LMs is the production of a stable marble. Unlike bare droplets in air or closed microchannels, the addition of particle shells to the liquid-air interface enables LMs to operate with a durable working space. Numerous studies have been conducted to explore effective fabrication strategies for various LMs and investigate the detailed effects of coating particles on the overall marble performance[17–20]. However, there are still uncertain particulate factors that need to be taken into account in the formation of LMs. The haphazard arrangement of particles during manual rolling not only affects the production efficiency of LMs, but also frequently yields non-uniform and disorderly shells, resulting in the inadvertent loss of a considerable number of coating particles. Moreover, accumulation of surplus coating particles may not facilitate the prevention of liquid core evaporation and could, to a certain extent, further impede the transport and sensing of LMs[21,22]. Generally, the distribution of coating particles impacts not only the lifespan of LMs on various substrates but also the coalescence and splitting of multiple LMs containing reactant essences. This necessitates the fabrication of LMs featured by single layer coverage with uniform particle distribution.

[1]School of Mechanical Engineering and Automation, Harbin Institute of Technology, Shenzhen 518055, China. [2]School of Science, Harbin Institute of Technology, Shenzhen 518055, China. [3]School of Energy and Power Engineering, Shandong University, Jinan 250061, China. [4]These authors contributed equally: Jing Jin, Zheng Huang. ✉e-mail: jinjing2020@hit.edu.cn; chenhuaying@hit.edu.cn

However, due to the extremely low mass of coating particles employed and the daunting task of particle counting, achieving a defined coverage of LMs for broader use of LM-based miniaturized platforms is technically challenging. This paper puts forward a practical technique to construct stable LMs featured by monolayer structure with adjustable particle coverage rates, fulfilling the prerequisites of swift maneuverability and straightforward detection with fewer particles. First, selected polystyrene (PS) microspheres were treated hydrophobically to ensure excellent particle monodispersity. Then, a custom-made manufacturing device was created, comprising a rolling module and an injection module, for producing variable LMs on demand. Subsequently, we investigated the face profile, particle distribution and maximum volume of formed LMs in detail, after clarifying the well-defined monolayer structure. To evaluate the performance of these marbles, a series of experiments were systematically conducted on investigating their behavior in rotation, compression, evaporation and coalescence, from both static and hydrodynamic perspectives. Furthermore, the potential applications based on flexible LMs were demonstrated through diffusion reaction and cleaning experiments at the mesoscopic scale. The study presented here aims to shed new light on exploring the potential LM-based miniaturized platforms have for future applications, especially for parallel biochemical analysis and point-of-care testing.

Results and Discussion

Monolayer LMs prepared by modified PS microspheres

In essence, LMs are a variant of droplet microsystem with a core-shell structure that necessitates the incorporation of appropriate coating particles. Due to the spontaneous assembling process and different properties of particles, handcrafted LMs have a multi-layered shell and are frequently accompanied by particle aggregation, which increases the unnecessary particle consumption. For obtaining stable LMs with fewer particles, precise controlling of the particle distribution on these LMs is essential. However, due to the possibility of excessive dispersion of the particles aggregated in multiple layers under minor disturbances, it can be technically challenging to control. Therefore, a stable LM with the shell of monolayer structure is highly sought after, where stringent requirements including excellent monodispersity, low cohesion and large size are often put on its coating particles[19,23]. Considering these, this study encompasses various coating particles, differing in type and size, to produce a wide range of LMs, as depicted in Supplementary Fig. 1. Finally, 50-μm PS microspheres were selected after systematic cross-experiments on choosing appropriate coating particles, based on their good compatibility and suitable particle size. While both hydrophilic and hydrophobic particles can be used to create LMs[24–26], the hydrophobic variant is typically more favorable in producing stable LMs, particularly for monolayer LMs.

To enhance the hydrophobicity of 50-μm PS microspheres, we employed a mixed hydrophobic treatment agent, as demonstrated in Fig. 1a. The hydrophobic agent can effectively form a thin film (~ 100 nm) on a glass slide surface after drying, resulting in a significant improvement of substrate hydrophobicity, as shown in Supplementary Fig. 2. The expected PS microspheres with satisfactory hydrophobicity were eventually obtained following a thorough surface treatment employing the dip-coating method shown in Fig. 1b. It is noteworthy that the mass ratio of raw particles to the hydrophobic agent should be controlled at about 1/4. Inadequate usage of the hydrophobic agent leads to insufficient hydrophobicity of the treated PS microspheres, resulting the failure of marble formation. On the flip side, an excessive amount of the agent often generates numerous block film fragments that can exist as impurities, which are hard to eliminate and may cause an undesired increase in size. Furthermore, for better hydrophobicity, the resting time of treated particles should be more than 24 h. Insufficient hydrophobicity and block film fragments may reduce the particle mobility on the liquid-air interface, greatly preventing the formation of stable LMs with fewer particles. The effectiveness of particles treatment can be evaluated by injecting liquid content into a LM. When the shell particles appear to be separated in lumps rather than moving downwards in a tightly packed arrangement during the injection process, it indicates that these particles do not satisfy the demand (see Supplementary Fig. 3, discussed in Supplementary Note 1).

Compared to the untreated PS microspheres, the surface of treated microspheres displayed a noticeable increase in roughness while maintaining good monodispersity and low cohesion, Fig. 1c. Following this, a 10-μL bare droplet was dropped and manually rolled on a powder bed of loose PS microspheres. The corresponding LM could be readily constructed within a few seconds with remarkable stability on both solid and liquid substrates, as shown in Fig. 1d. Here we firmly define the radius of the LM as that of the bare droplet because of the relatively small ratio between the particle and droplet radii. Notably, the droplet core left distinct imprints on the powder bed during manual rolling, indicating the successful detachment of microspheres from the bottom after momentary contact.

For a LM exhibiting an ellipsoidal shape with limited deformation, the detailed distribution of particles around the droplet core is crucial for its lifespan and could be determined numerically. The top- and side-view images of a 10-μL LM in Fig. 2a clearly show the compact organization of modified PS microspheres on the liquid-air interface, without any additional microspheres outside the marble contour line. Assisted by optical microscopic observation, we discovered the tightly packed hexagonal arrangement of microspheres at the marble bottom from Fig. 2b, with no visible particle stacking. Moreover, we assessed the invasion of PS microspheres into the surface of a sessile LM by delicately altering the observation angle. The microspheres consistently maintained similar invasion depths, indicating a uniform hydrophobic treatment to these particles. More importantly, only a thin particle layer with a rough thickness δ of 45–55 μm can be observed on the liquid-air interface, Fig. 2c. These results strongly confirm the exceptional performance of hydrophobically treated PS microspheres and their great efforts in preparing stable LMs encased in a monolayer particle shell. The use of PS microspheres avoids the complex substrate modification required for preparing monolayer LMs when using SiO_2 or PMSQ particles[18,19]. The hydrophobic treatment of PS microspheres improves the stability of monolayer LMs we produced, which is the basis for further reduction of particle consumption. Furthermore, we analyzed the distribution of PS microspheres at the bottom of sessile LMs *via* image labelling analysis, as depicted in Fig. 2d. After labelling the target microspheres within a set of arbitrary hexagonal boxes, the relative proportion of granular area was quantified respectively from 400 captured images using the pixel recognition function in MATLAB. The mean surface area proportion occupied by PS microspheres in a single marble was calculated as 0.865, which slightly deviates from the result (0.906) obtained by the same method in the calculation of the ideal hexagonal arrangement (more details in Supplementary Fig. 4, discussed in Supplementary Note 2). This finding greatly supports the conclusion that the LMs synthesized in this study feature a monolayer configuration within their shells. Consequently, a batch of stable monolayer LMs encapsulated by hydrophobic particles can be prepared for future use.

Volume expansion of LMs through direct liquid injection

To achieve accurate controlling of the particle distribution in a monolayer LM, the number of coating particles lying on the droplet surface needs to be predetermined. Nevertheless, the minimal amount of particles needed to form a single marble makes direct weighting or thermogravimetric analysis impractical, due to potential accuracy loss and environmental limitations. Now turn the question around and we can see that the porous shell structure of LMs allows for direct injection as a viable option for easily changing the liquid volume. Therefore, instead of tallying coating particles, we can expand the volume of the droplet core, while maintaining the initial coating particles on the liquid-air interface. Based on the morphological change observed in the continuous volume expansion process in Fig. 3a, the expanded LMs were found to approach deformed ellipsoids and manifest greater opening areas on their surfaces. The diverse opening areas of these LMs with 3D interior structure offer significant convenience for reagent addition or removal and real-time monitoring in droplet-based microreactions. For the marble volumes used in this study, the corresponding Bond number Bo was found

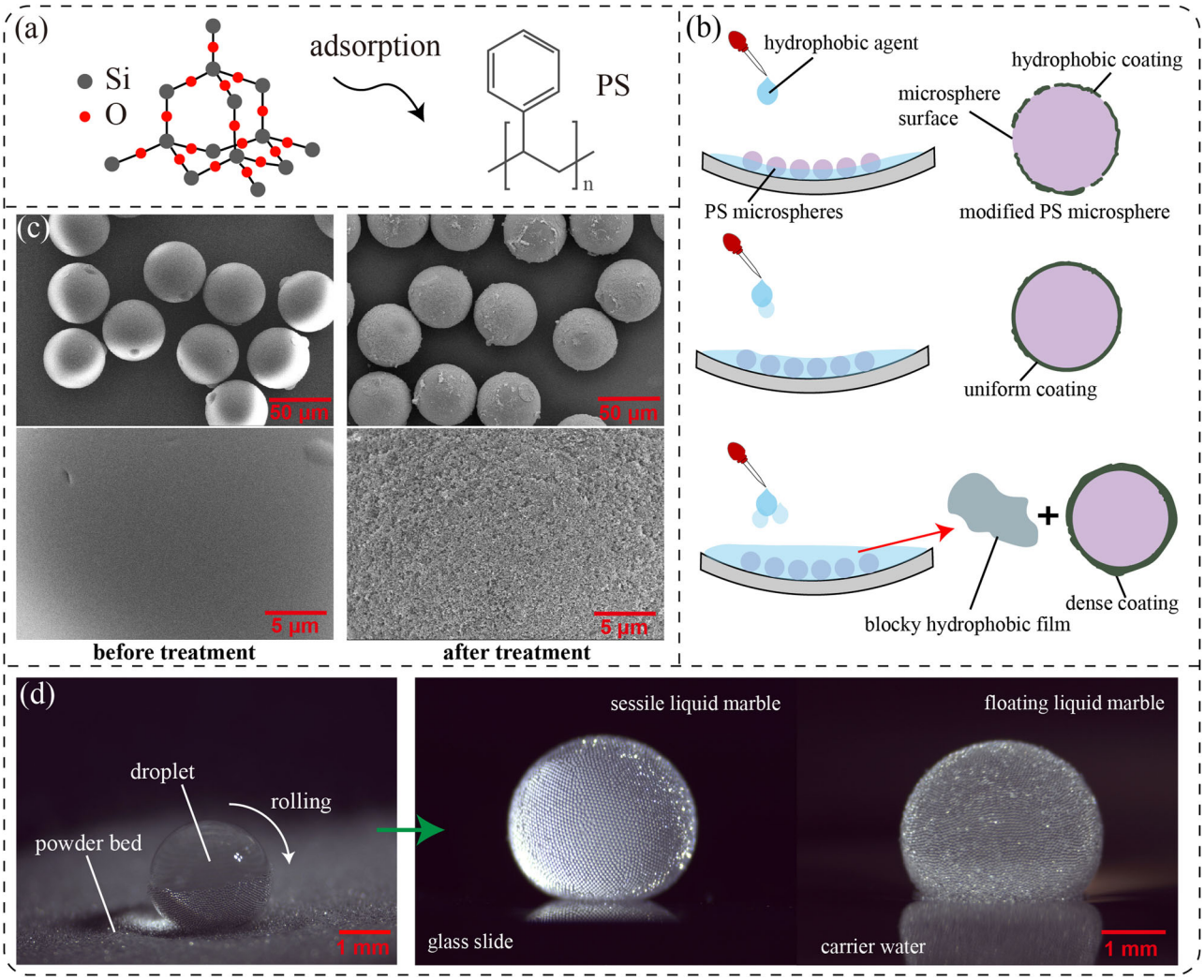

Fig. 1 | The process of particle treatment and formed LMs. a Schematic of the combination between silane and PS microspheres. **b** Schematics of PS microspheres treated with inadequate, moderate and excessive amounts of hydrophobic agents. **c** Micrographs of PS microspheres before and after fine hydrophobic treatment. **d** The production process of a 10-μL LM and stable LMs resting on solid and liquid substrates respectively.

to be much smaller than 1 (see Supplementary Fig. 5, discussed in Supplementary Note 3). The surface tension of the droplet core and the effect of particulate interaction dominates together a monolayer LM approaches to a near-spherical shape at its initial volume. As the droplet volume increases, Bo increases, and gravity begins to take over, resulting in the half-opened LM gradually becoming flatter but still steric[16].

We collected a series of side-view images of sessile LMs with fixed volumes ranging from 10 to 50 μL and computed their corresponding surface areas by using two geometric models (namely ideal ellipsoid model and deformed ellipsoid model) and the numerical solution of the Young-Laplace equation, as displayed in Fig. 3b. It is clear that as the volume of LMs increases, they can no longer be treated as rigid spheres and the spherical surface area deviates significantly from the actual value, necessitating the use of more accurate models. It is worth to note that the surface area discrepancy between the ideal and the deformed ellipsoid models is minimal, despite the common belief that the latter model with a missing cap bulk is a better approximation of reality. Besides, solving the Young-Laplace equation is another feasible method, which generally involves with several boundary conditions such as marble contact angle and surface tension of water droplet. Although the equation solution fits the actual shape of LMs well and its calculation results are very close to those of the deformed ellipsoid model, as shown in Supplementary Fig. 6, there may still be slight deviations from the true value. This is because that the effective surface tension of the LM should be used in solving the Young-Laplace equation to obtain more realistic results[27]. Therefore, for convenience, especially to avoid repeated measurements of the contact angle and complicated calculations of the effective surface tension of LMs, we directly selected the ideal ellipsoid model for fitting the curve of marble volumes and corresponding surface areas. To validate this assertion, the detailed surface area ratios of randomly selected marble volumes were calculated by experimentally analyzing their side-view images, with a particular focus on the shell edge lines. The obtained values were intriguingly found to be similar to, or slightly higher than, the theoretical values estimated from the curve of particle area proportion relative to the volume ratio, as demonstrated in Fig. 3c. The higher proportion of particle area observed here should be attributed to the irregular increase in microspheres gaps during volume expansion and insufficient particulate information from random side-view images.

In addition, it has been noted that LMs with malleable coatings can stably exist on hydrophilic surfaces, and even on carrier liquids, despite their volume expanding to several times greater than the initial volume. We hold the belief that the protective mechanism arises from the redistribution of microspheres on the liquid-air interface. As the volume of a sessile LM increases, more microspheres continuously gather in the lower part of the marble due to the synergistic effect of gravity and microflows, providing sufficient coverage for the enlarged surface area, as illustrated in Fig. 4a. According to this mechanism, the maximum survival volume can be

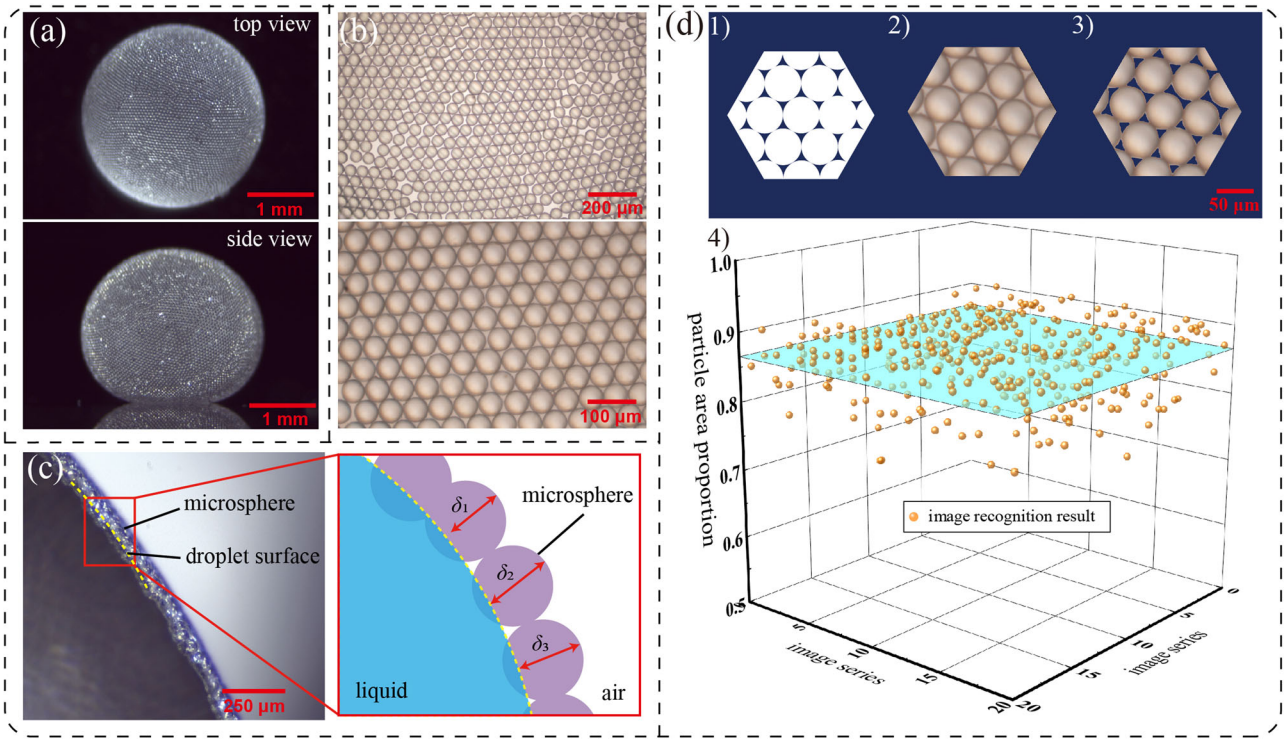

Fig. 2 | Monolayer particle shell characterization. a The top- and side-view images of a 10-μL LM. **b** Micrographs of tightly packed microspheres at the bottom of a sessile LM. **c** Schematic of the invasion status of single-layer microspheres on the liquid-air interface. **d** Illustrations of 1) the theoretical arrangement, 2) the experimental arrangement and 3) the labeled arrangement of PS microspheres, as well as 4) the image recognition results of particulate area proportion in LMs.

predicted when the critical bottom area of the expanded LM is exactly equal to the total surface area of the original LM before rupture. Nevertheless, the largest volume that LMs with initial volumes of 5, 10, 15, and 20 μL can survive is respectively 60, 100, 135 and 150 μL on average, corresponding to a significantly smaller critical bottom area than the surface area of unexpanded counterparts, as shown in Fig. 4b. The discrepancy is likely due to the uneven shell edges caused by the individual difference of microspheres, as depicted in the upper images of Fig. 4c. Although asymmetric microflow is unavoidably generated during liquid injection, its impact is limited, as shown in Supplementary Fig. 7. The edge of the protective shell, resembling a flying carpet, results in the presence of the "barrel effect". When the droplet core around the "short board" is exposed to a hydrophilic substrate due to disturbance, the expanded LM ruptures immediately. This effect is particularly pronounced in large-volume LMs that are more susceptible to wobbling from minor perturbations.

It is worth noting that the gap between the bottom microspheres does not increase infinitely during the process of volume expansion, as shown in the images at the bottom of Fig. 4c. In this period, the microsphere spacing at the bottom initially increases and may even develop some visible cracks. Nevertheless, the utilization of hydrophobic PS microspheres here ensured that the droplet core remained at a specific distance from the carrier substrate, effectively preventing any physical contact[18]. At the beginning, the total surface area of an individual LM varied significantly with its volume, resulting in a strong splitting effect. Gradually, however, as the volume increased, the growth rate of the surface area decreased, eventually leading to a reduction in the splitting effect, Fig. 4d. We further carried out force analysis on selected bottom microspheres during volume expansion, considering three forces, namely van der Waals force, friction force and lateral capillary force, as depicted in Fig. 4e[28–30]. The effect of van der Waals force is not taken into account at long distances, as it is a short-range force. The lateral capillary force usually prevails over the electrostatic force, which contributes to holding the gap between microspheres from expanding[17]. The movement of microspheres is always constrained by the friction force, which is proportional to the marble volume. In this study, van der Waals and lateral capillary forces extensively exist between closely packed microspheres, preventing the migration of these microspheres during volume expansion. In contrast, the same forces have been weakened with the intervention of a strong splitting effect, which gradually fails to impede microsphere migration. Consequently, the gap between the microspheres at the bottom widens in general at first. As the marble volume continuously expands, the friction force plays an essential role in maintaining a consistent microsphere gap, while the splitting effect is receding. In addition, the microspheres within the proximity of small cracks were found to have a delicate force balance. Benefiting from this, small cracks do not increase in size dramatically during volume expansion. However, a gentle shaking process can disturb the equilibrium. During shaking, a part of the lower surface of an expanded LM could be lifted temporarily, allowing the PS microspheres that were previously held in place by the droplet's gravity to move and fill the resulting gaps (more details in Supplementary Fig. 8, discussed in Supplementary Note 4). This also confirms the exceptional hydrophobicity and flowability of PS microspheres.

Hydrodynamic analysis on rolling LMs with different coverage rates

Here we disregarding the inherent particle spacing in the monolayer arrangement of microspheres and set the relative particle coverage rate of the initial LMs with an average particle area proportion of 0.865 to 100%. Thus, the detailed coverage rate of expanded LMs can be obtained from the ratio of initial surface area to the corresponding enlarged surface area (S_0/S). Through directly liquid injection, we have achieved the controllable preparation of LMs with a broad range of particle coverage rates, ranging from 20% to 90%, in increments of 10%. While the aforementioned LMs with adaptable coverage shells demonstrate stable survival, research indicates that particle coverage ranging from 50% to 90% is a reasonable motion range after systematic kinetic validation. In cases of gravitationally triggered motion of partially covered LMs, those marbles with clear opening areas did not rupture, but instead rolled at a certain speed, as depicted in Fig. 5a. To the best of our knowledge, this unique phenomenon has not been

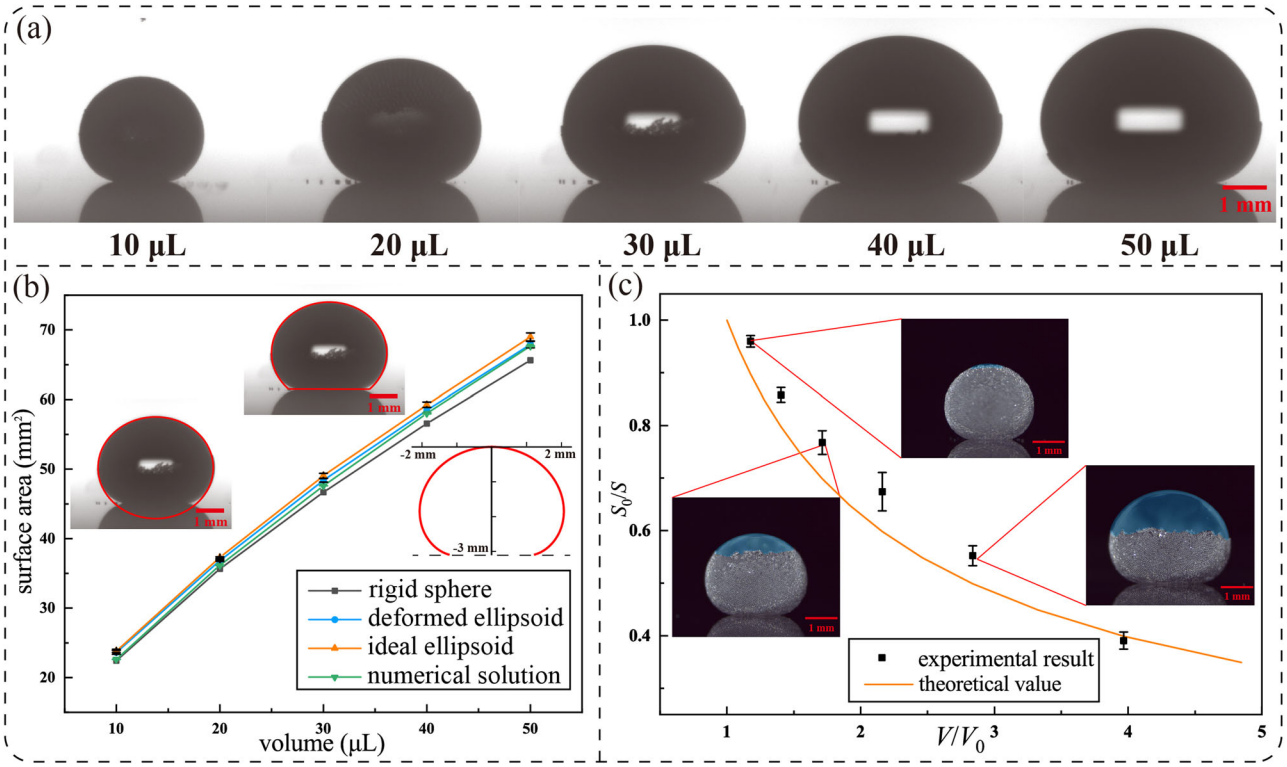

Fig. 3 | Control of surface particle distribution. a The morphological change of a sessile LM during volume expansion. **b** The relationships between volumes and surface areas of expanded LMs in different calculation methods. **c** The comparison of inverted surface area ratio S_0/S between the theoretical values obtained from an ideal ellipsoidal model and the experimental results estimated by shell edge detection at different marble volume ratios V/V_0. Error bars represent the sample standard deviation.

documented in prior studies. We assume that this self-protective mechanism stems from the extraordinary locomotivity of microspheres situated on sessile LMs. Moreover, it has been observed that LMs with different coverage rates exhibit opposite phenomena, namely rupture and escaping, at the end of the rolling motion. Thus, we believe that the mechanism should have limitations due to the fact that the increasing opening area around the bottom of rolling LMs exposes to the external environment over time. To investigate this further, a large number of experiments were conducted to determine the velocity limitation of variable LMs *via* a gravity-driven approach. The data shown in Fig. 5b reveals that the rupture velocity for LMs with coverage rates at 50%, 60% and 70% is 67.68, 72.65 and 59.70 mm/s, respectively. On the other hand, the escaping velocity for LMs at 80% and 90% coverage rates rise to 131.72 and 121.98 mm/s. The rupture velocity initially increases with the coverage rate, but unexpectedly decreases at around 70%. However, once the coverage rate reaches 80% or more, the opened LM no longer experiences breakage, but instead rushes out of the finite inclined surface plate at high velocity.

Based on the unusual trend in velocity observed, we conducted further research by employing a high-speed color camera to examine the movement details of coating particles. During droplet rolling, surface particles continuously tumble from bottom to top and redistribute on the surface due to combined action of gravitational effect and droplet microflow, forming a particle cushion for the advancing droplet core. It is deduced that the self-protection mechanism of opened LMs can be divided into two categories according to the detailed particle coverage rate, as presented in Fig. 5c. A value below 70% indicates low coverage rate and the corresponding mechanism can be described as "tracking protection". Under this mechanism, hydrophobic particles with a remarkable flowability prefer to move freely towards the bottom blank region of a partially covered LM, fulfilling the guarding task of droplet core before it encounters the substrate. The opening window always stays at the anterior end of the LM, enabling it to roll like a colossal phagocyte that engulfs foreign matters in its path. A coverage rate exceeding 70% is considered high. It establishes a "scattering protection" mechanism while maintaining the functionality of "tracking protection". The restricted opening area of high-coverage LMs can be replenished with other particles nearby, forming a protective barrier in rolling. This effect persists even if the gap between the embedded PS microspheres widens somewhat. In general, an opened LM with sufficient shell coverage displays exceptional motility and facilitates the simple addition of reagents, overcoming the limitation associated with external field-induced particle motions. Notably, the 70%-coverage LM could represent the transition state from low to high coverage, with a protective mechanism quite similar to that of the high-coverage LM. However, the protection effectiveness of shell particles is diminished, as the surrounding particles cannot complete the wrapping in time due to the large opening area. Simultaneously, they excessively consume the particles necessary for "tracking protection", leading to a premature fragmentation. Moreover, it has been observed that the alteration of activation angle produces an unforeseen shift in the protection mechanism of opened LMs. For instance, when the activation angle increases to 42', the rupture velocity of a 60%-coverage LM decreases dramatically to only 61.43 mm/s, as illustrated in Supplementary Fig. 9. For higher activation angles, the hydrophobic microspheres at the top of the LM tend to flow back towards the opening area much easier, potentially resulting in the advancement of the transition zone.

There is a significant difference in the rupture distance of these LMs with similar opening areas, as depicted in Fig. 5d. Specifically, 50%- and 60%-coverage LMs rupture at around 200 mm from the starting point, while the 70% counterpart breaks at approximately 100 mm, which is mainly attributed to distinct friction impacts. As a particle-covered droplet system, the friction of LMs on any solid substrates bear a significant resemblance to that of bare droplets on a superhydrophobic surface. In addition, most LMs will undergo pinning-depinning transitions when rolling, primarily due to their unique particle shell structure. As a result, their friction mechanism is

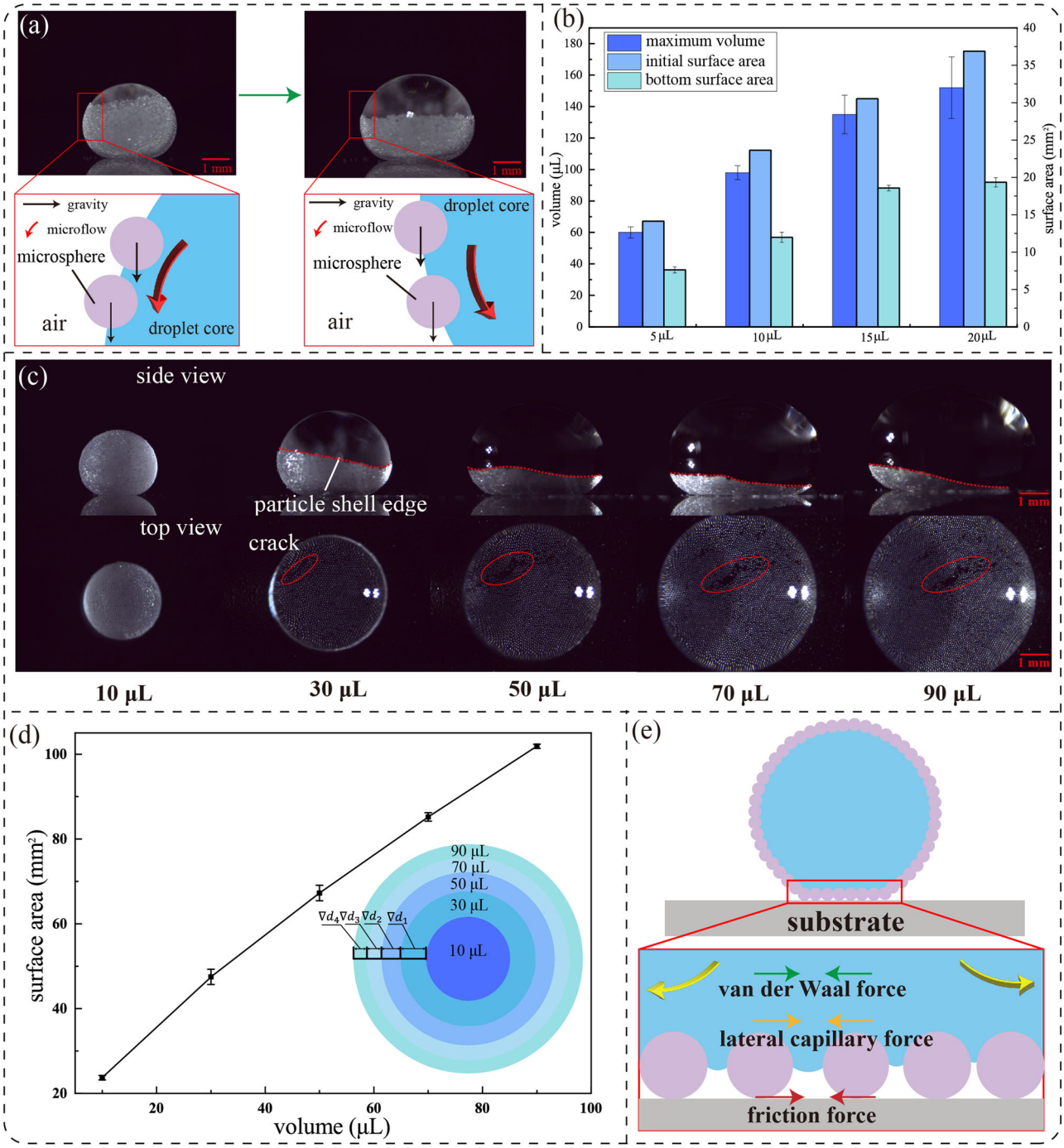

Fig. 4 | Distribution of surface particles during liquid injection. a Schematics of microsphere motions during volume expansion. **b** The comparison of maximum survival volume, initial surface area and the corresponding bottom surface area for different original LMs. **c** The development processes of lateral shell edge and bottom crack formation during volume expansion. **d** The relationship between total surface area and marble volume in a wide range of LMs (Inset: schematic diagram of enlarged bottom surface areas). **e** Schematic of the close interaction of coating particles underneath. Error bars represent the sample standard deviation.

dominated by the energy dissipation caused by the detachment of the three-phase contact line. Based on this, any increase in the rolling velocity of LMs will lead to a faster cycle of pinning-depinning transition, which in turn accelerates the energy dissipation in LMs, for instance, the acceleration due to the change of gravity component. Furthermore, it should be noted that the friction of LMs is directly proportional to the perimeter of the three-phase contact line[31,32]. This analysis is consistent with our findings that as the volume of LMs increases, the particle coverage rate decreases, while the corresponding circumference of their three-phase contact lines lengthens. This leads to a steady acceleration increase with the coverage rate of expanded LMs before rupture, resulting in a substantial variance in rupture distances.

In addition, the activation method is instrumental in determining the ability of opened LMs to fulfil multiple rotations. This study has identified two gravity-based activation methods controlled by an angle regulator. The first method involves a gradual increase in the activation angle until a sessile LM starts to roll, minimizing undesirable interference and granting microspheres ample time to shift to the front side of its droplet core under the influence of gravity. By utilizing this approach, the critical coverage rate of LMs for motion was reduced to 40% or less. Alternatively, there is an

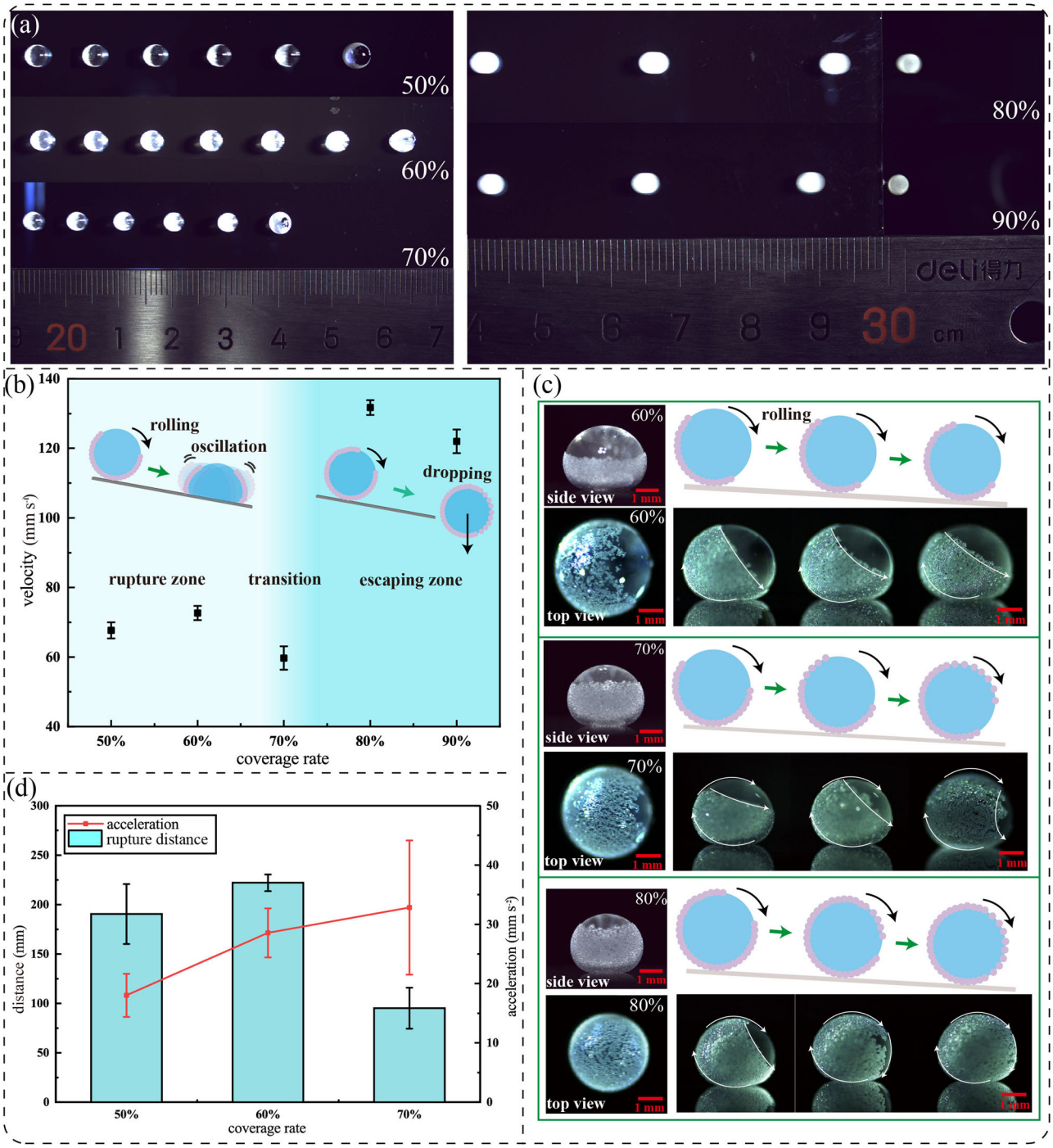

Fig. 5 | Dynamic characterization of LMs with opening areas. a Different trajectories of flexible LMs rolling on a finite surface plate. **b** Critical velocities of rupture and escaping motions for 50%–90% coverage LMs on an inclined plate (activation angle: 36′). **c** Snapshots and schematic illustrations of self-protection mechanisms for low-coverage, transition state, and high-coverage LMs. **d** The rupture distance and the corresponding acceleration for 50%, 60% and 70% LMs in rolling motions. Error bars represent the sample standard deviation.

approach that involves instant startup, where the motion of LMs starts by rapidly increasing the angle to a default value. However, this tactic may cause substantial disruption and may even give an upward momentum to a stationary marble. Consequently, when implementing this method, the coverage rate of activated LM can only achieve a minimum of 50% or slightly more. Following this, we conducted further research on the activation angle of LMs with different coverage rates under the slow startup method, as depicted by Fig. 6a. Undoubtedly, the variance in the activation angle is closely relative to different marble volumes. By measuring the alteration between the advancing and receding contact angles, the motion of an LM on a level surface can be quantified, as shown in the inset of Fig. 6a. The movement of the sessile LM begins when the difference exceeds the hysteretic contact angle[33]. This angle difference can be created by introducing an inclined plane, with the inclination angle of the plane needed being inversely proportionate to the marble volume[34–37]. Surprisingly, the activation angle for 100%-coverage LMs was quite high (up to 1°24′), which could potentially be attributed to the flow-obstructed particle shells impeding the development of advancing and receding contact angles. Furthermore, we measured the corresponding rupture velocities of opened LMs activated by different methods and found them to be very similar, as shown in Fig. 6b. The

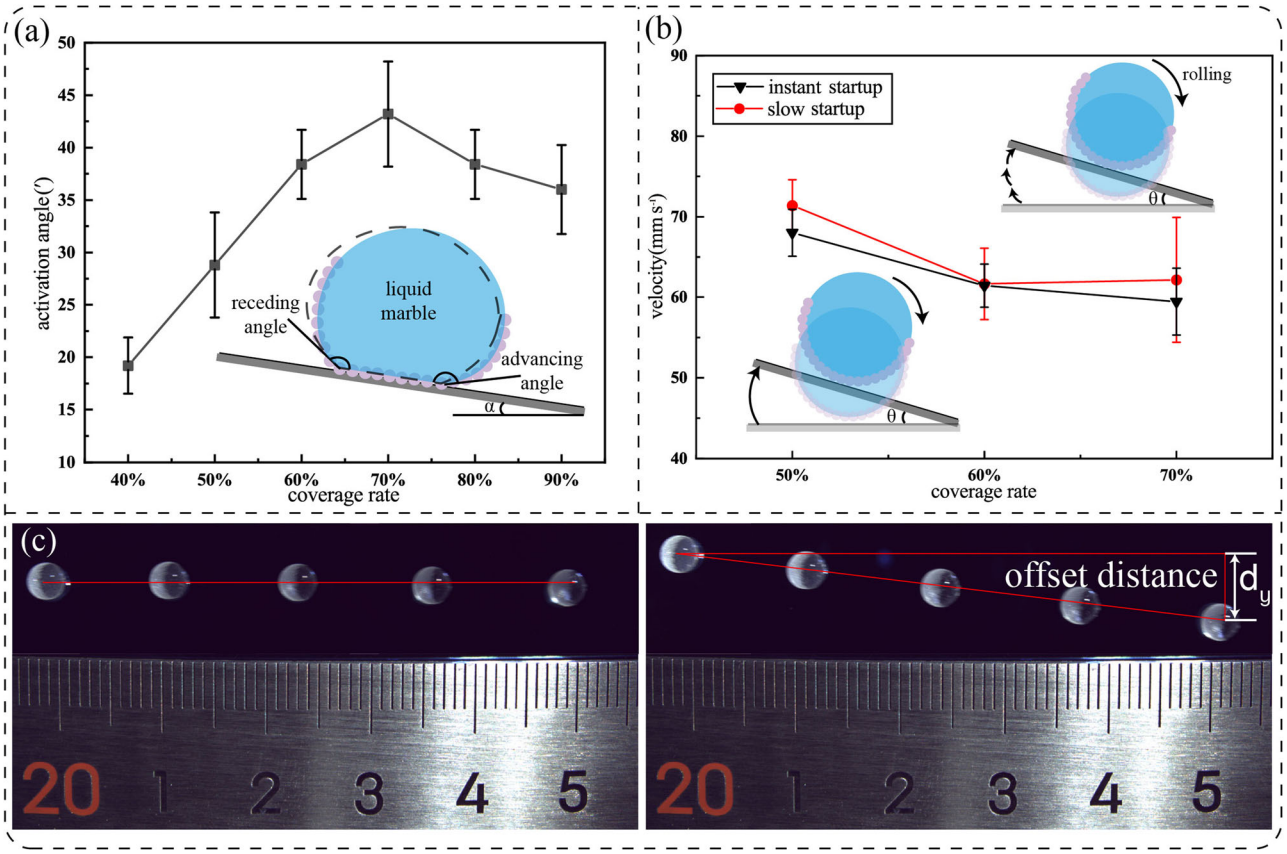

Fig. 6 | Effects of the activation angle and startup pattern on marble rolling. **a** The activation angle of opened LMs with 40%–90% coverage in slow startup (Inset: schematic of a sessile LM on an inclined plate). **b** The rupture velocities of 50%-, 60%- and 70%-coverage LMs in slow startup and instant startup patterns. **c** Image sequences of the straight and diagonal motions of opened LMs when rolling. Error bars represent the sample standard deviation.

aforementioned observation suggests that the disturbance induced by instant startup solely impacts short distances, and does not endure throughout the movement of LMs. It is of importance to note that the opened LMs exhibit diverse degrees of deflection as they move, as represented in Fig. 6c. We presume that this phenomenon is related to the distribution of microspheres on the surface of LMs. Specifically, the irregular distribution of the microspheres leads to their motions being uneven relative to the droplet core, ultimately resulting in the deflection.

Robustness and various functions of flexible LMs

The robustness of LMs plays a vital role in determining their practical viability. The ability of LMs to maintain stability on hydrophilic surfaces distinguishes them from bare droplets. This study examines the mechanical stability of sessile LMs with different coverage rates between a hydrophilic substrate as the base and a hydrophobic substrate as the ceiling, which intends to provide a reference for selecting suitable LMs at a relative low cost, as illustrated in Fig. 7a. With a group of coverage rates from 50% to 100%, the corresponding LMs were compressed smoothly and found to collapse at their highest normal pressure point, which differs a lot and rises up as the coverage rate increases, Fig. 7b, c. Despite the apparent nature of this result, the breakage principle of the LMs varied significantly (more details in Supplementary Fig. 10, discussed in Supplementary Note 5). LMs with wide transparent openings were frequently damaged due to the uneven growth of the particle shell, causing the droplet core to interact with the hydrophilic substrate. This is also the reason for the substantial disparity in critical pressure among individual LMs. The principle of breakage for the fully covered LMs differs slightly. The breakage is not caused by greater spacing between bottom particles, but rather by droplets within cracks formed by the expanded surface area during the squeezing process. For LMs with limited opening areas, their breakage principle is quite similar to that of fully covered LMs as they tend to be protected by the hydrophobic ceiling plate in the inhomogeneous development of particle shells. For instance, the difference in the opening area of 60%- and 70%-coverage LMs leads to a notable discrepancy in their respective critical pressure, as illustrated in Fig. 7b. Additionally, these opened LMs demonstrate remarkable elasticity. The marbles manifested swift recovery even when deformed close to their breaking point, whereas the LMs with complete coverage exhibited significant deformation upon release of pressure near the point of fracture.

Besides, the lifespan of LM-based microreactors is significantly impacted by the evaporation of LMs. A small volume of LMs results in a short usage time, whereas increasing the volume leads to a waste of resources. A viable solution to this dilemma is to use LMs with an opening area through volume expansion, which have a longer service life and a certain degree of mobility. The extended service life (the time period before recovering to full coverage) of the LMs can be regulated by controlling the expansion volume. It should be noted that the evaporation rate of LMs will be accelerated as the opening area increases, as shown in Fig. 7d. Moreover, there is evidence that the rate of particle coverage can be reversed, as demonstrated by the recovery of the opened LMs. This occurred by starting from low coverage and returning to 100% while the droplet core evaporated, as illustrated in Fig. 7e. Therefore, a series of flexible opened LMs may be produced for future use after fine evaporation control. As the core droplet continues to evaporate, the LM will gradually collapse, resulting in the shedding of coating particles for the production of low-dimensional nanomaterials.

Merging of LMs requires overcoming the obstacle of rigid particle shells, which usually requires a considerable amount of energy[38,39]. In this study, we aimed to fuse LMs with different coverage rates to determine the critical merging condition. Our findings show that a 90%-coverage LM cannot effortlessly blend with another LM due to its relatively small opening

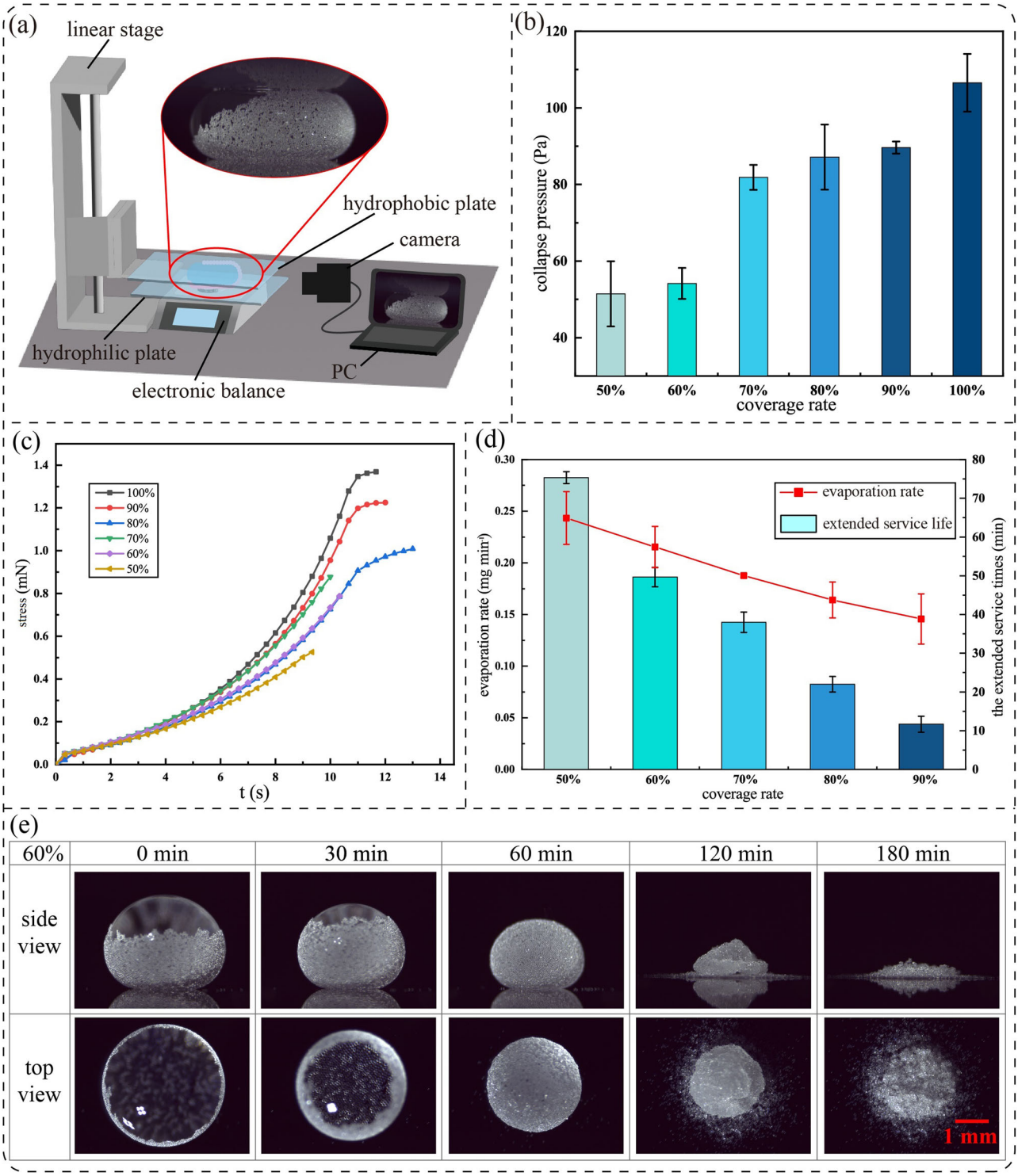

Fig. 7 | Stability and service life of LMs with different opening areas. a Schematic of the experimental setup for squeeze test. **b** Collapse pressure of LMs with different coverage rates. **c** Illustration of the normal force evolution in squeezing. **d** The extended service life and the evaporation rate of LMs with opening areas. **e** Image sequences of the morphological change of a 60%-coverage LM during evaporation. Error bars represent the sample standard deviation.

area, as shown in Fig. 8a. However, as the particle coverage rate decreases, fusion becomes easier. For instance, two LMs with 50% coverage may merge easily with minor air turbulence. Besides, merging two LMs with different coverage rates can be a promising way to regulate the particle distribution on the liquid-air interface. As depicted in Fig. 8b, two LMs with 80% or lower coverage rate typically merge, resulting in a fused LM with a higher coverage rate that may exceed 100%. This function is highly advantageous in biochemical applications as ample coverage affords effective safeguarding, a crucial factor when efficiently encapsulating sensitive substances or hazardous reaction byproducts. Furthermore, LM coalescence induced by this method can create Janus marbles with great effectiveness. A Tai Chi patterned Janus LM can be generated through fine control of the merging process, as seen in Fig. 8c. This provides a promising option for the restricted selection of Janus LM fabrication strategies currently available[40,41]. Moreover, an array of valuable applications can be explored based on the diverse properties of the flexible yet stable LMs produced in this study. For instance,

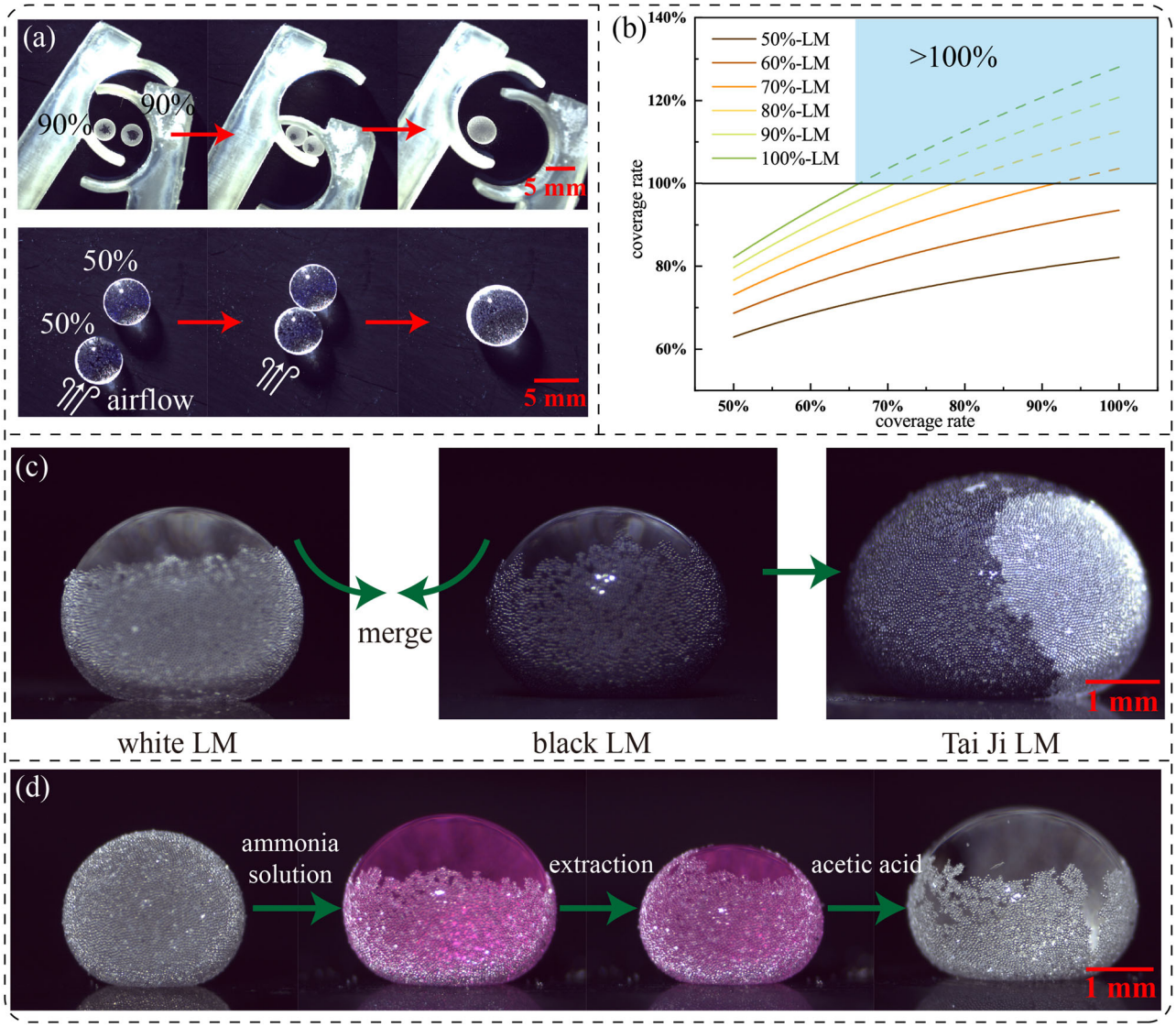

Fig. 8 | Merging and applications of various opened LMs. a Snapshots of the merging process of two LMs with the same coverage rate. **b** The operation map for regulating particle coverage rate by fusing two LMs with different coverage rates. **c** The formation of a Tai Chi patterned Janus LM. **d** The color change process of acid-base neutralization reactions inside LMs.

LMs equipped with opening windows enable direct observation of their inner space, facilitating real-time monitoring of any reactions occurring within, as demonstrated in Fig. 8d. It is noteworthy that the reaction liquid can be effortlessly extracted whenever necessary. The self-cleaning features of solid surfaces have generated considerable interest for their extensive practical applications[42–44]. Nonetheless, hydrophobicity is often a prerequisite for solid surfaces to implement self-cleaning work by trapping surface contaminants in directional droplet rolling motions[45,46]. In contrast, hydrophilic surfaces are difficult to cleanse due to residual liquid residue. However, Supplementary Fig. 11 illustrates that LMs with openings are partially capable of cleaning hydrophilic surfaces, which presents an innovative option for surface cleaning research.

Conclusions

This paper presents a straightforward and effective method for fabricating monolayer LMs with adjustable particle coverage rates. First, PS microspheres with an average diameter of 50 μm after hydrophobic treatment were selected to encase water droplets, resulting in stable LMs with visible monolayer structures. Aided by a custom-built injection platform, it is easy to obtain LMs with particle coverage rates ranging from 20% to 90% *via* volume expansion. These flexible LMs featured by clear opening areas demonstrate excellent stability, both on solid and liquid substrate surfaces, despite an increase in volume up to several times their original size. Moreover, the study reveals that a higher particle coverage rate between 50% and 90% is reasonable for gravity-driven rolling motions. Based on the rupture phenomenon observed for low-coverage LMs and the escaping phenomenon observed for their higher counterparts, two self-protection mechanisms with a transition zone have been proposed to explain the opposite results aforementioned. In normal compression experiments, the expanded LMs exhibit a resilience similar to that of bare droplets, albeit with the fact that the marble stability decreases at lower coverages. The use of opened LMs offers an effective solution to the challenges posed by the rigid particle shell during merging and presents a practical approach for the secondary regulation of LMs' coverage rates. Furthermore, these opened LMs tend to have a longer lifespan than fully covered LMs due to the expansion of the droplet core. This study also emphasizes the 3D visualization feature and cleaning capability on hydrophilic surfaces of these expanded LMs. Our study has enhanced our knowledge of the family of LMs and uncovered their overall characteristics. It provides a reference for the green application of stable LMs, offering insightful perspectives for further

research on LMs and urges researchers from various fields to pay attention to these independent particle-laden droplet microsystems. The combination of flexible shell-covered LMs with superhydrophobic surfaces appears attractive and can facilitate the safe and precise handling of small-volume droplets. Researchers should take note of the programmable handling of flexible LMs on different substrates to fully exploit the benefits of 3D reaction chambers. It is advisable to employ more efficient detection techniques for realizing real-time monitoring of the internal processes, providing a potential solution for multifunctional LM-based miniaturized platforms.

Methods

Selection and modification of coating particles

PS microspheres (10, 30 and 50 μm) were purchased from Wuxi RigoR Biotechnology Co. Thereafter, a simple dip-coating method was employed to hydrophobize all the microspheres. The microspheres were placed into a dish with a concave surface and then stirred gently after dropping an appropriate amount of mixed hydrophobic agent purchased from SOFT99 Co. (Glaco Mirror Coat Zero, containing alcohols and silica). The mass ratio of raw particles to hydrophobic agent could be controlled at about 1/4. After drying in the ambient environment for over 24 h, the hydrophobic microspheres could be detached by gently scraping them from the dish's surface. Subsequently, these modified PS microspheres were observed under an inverted optical microscope (Olympus Co., IX73) and characterized by scanning electron microscopy (Thermo Fisher Scientific, Apreo 2 S HiVac).

Fabrication and characterization of monolayer LMs

Non-wetting LMs were simply prepared by rolling discrete water droplets over a powder bed of modified PS microspheres until there was no trace of particle adhesion. Deionized water (18.2 MΩ·cm, 25 °C) was sourced from an ultrapure water purification system (Merck KGaA). Following systematic pre-experiments, 10-μL LMs were found to show remarkable structural integrity with minimal deformation and were particularly convenient for volume expansion calculations. Accordingly, we selected them as the control group for subsequent experiments. The profile of a static LM was captured from top and side views using a set of CMOS cameras manufactured by Shenzhen Jinghang Technology Co. Ltd (JHUM1200s). Similar equipment can be used to synchronously monitor the invasion state of coating particles. Additionally, the previously mentioned optical microscope was used to capture microscopic photographs of the particle distribution at the base of sessile LMs. A rapid particle recognition method aided by image labelling technology was then developed to predict the particle area proportion from the extensive collection of micrographs. Based on the geometric features of the underlying particle distribution, the bottom-view images were initially divided into hexagons *via* a custom written MATLAB program (MathWorks, MATLAB R2021b). Then, the microspheres within the hexagonal region were labelled using Eiseg, a publicly available interactive segmentation auto-labelling tool provided by the PaddleSeg team, in order to generate the annotated microsphere distribution image. Finally, the average area proportion occupied by the labelled microspheres within the hexagonal region was computed using MATLAB.

Fine control over particle distribution

First, an original 10-μL LM on a glass slide underwent naked-eye inspection to ensure integrity. Next, the marble was shifted under a PE syringe equipped with a microneedle. By utilizing a linear stage (ZOLIX Instruments Co., Ltd, AK25A-6520CZ), the microneedle was vertically inserted into the surface of the LM for liquid volume expansion. Then the volume of injected liquid was precisely controlled by a syringe pump from Baoding Acmer Precision Pump Co. (DSC-B01), enabling the acquisition of LMs with varying volumes and clear opening areas. The static LMs were observed from a lateral perspective using the aforementioned CMOS camera, and thereafter analyzed with *ImageJ* (National Institutes of Health) to determine the corresponding surface area of LMs with volumes from 10 to 50 μL. By comparing the surface area of expanded LMs with the initial microsphere distribution of 10-μL LMs, one can easily calibrate the respective particle coverage rates of LMs with varying volumes. Subsequently, we investigated the maximum volumes that different LMs could survive on a hydrophilic surface by injecting liquid volumes into the corresponding original LMs continuously under the same injection platform.

Hydrodynamic analysis on expanded LMs in motion

The dynamic behavior of LMs with different particle coverage rates was investigated by monitoring their inclined rolling motions. After gentle preparation, the LMs were transferred with care to a hydrophilic plate clamped on top of the platform horizontally. An angle controller (ZOLIX instruments Co., Ltd, KSMG15-40) was then used to precisely control the plate inclination, enabling the LMs to roll freely under the effect of gravity. A CMOS camera with ample depth of field (Shenzhen Jinghang Technology Co. Ltd, JHUM504s-E) was positioned directly above the platform to capture the track of these rolling LMs, while a high-speed color camera (Photron Ltd, FASTCAM Mini UX100, ~2000fps) was employed simultaneously to record the entire process of the marble's movement from a side view.

Testing and functionality exploration of versatile LMs

For extrusion testing, a hydrophobized glass strip secured to a motorized linear stage (ZOLIX Instruments Co., Ltd, LA150-60) was utilized to squeeze various LMs that were situated on the hydrophilic glass slide. The glass slide was connected to a balance-weighing platform to enable accurate measurement of the force results. During normal compression experiments, an electronic balance (Shanghai Hochoice technology, HC1204, ~120 g) was used to measure the critical pressure value of marble breakage as the displacement linear stage was moved. In addition, for droplet evaporation testing, LMs with specific particle coverage rates were prepared continuously and placed on a flat plate at room temperature. Colorful CMOS cameras mounted horizontally were used to record the morphological changes of the LMs, due to the shrinking volumes, by taking photographs at fixed intervals.

When two stationary LMs with small openings are brought into proximity, they cannot be easily merged and require the squeezing with hydrophobic rods. In contrast, even a gentle airflow can trigger the fusion of two LMs with large opening areas, forming a liquid bridge that allows for safe merging. Theoretical analysis predicts that two LMs with any particle coverage rates can produce a merged LM with a changed coverage rate, facilitating the further observation of internal flows. Besides, the combination of two LMs with different colored coatings leads to the creation of a Janus LM. The ability of 3D visualization in opened LMs was proved by the discoloration reaction between acids, alkalis and the pH indicator. Ammonia solution (H_5NO, 25–28%) and acetic acid (CH_3CO_2H, 36%) were obtained from Shanghai Aladdin Biochemical Technology Co. Ltd. Phenolphthalein indicator solution (10 g L^{-1}) was purchased from Codow Co., which was first injected into a completely covered LM using the same injection platform aforementioned. Then, we added the ammonia solution to the marble for visualizing color changes. After extracting a certain volume of liquid from the expanded marble, the acetic acid was put into the LM for neutralization reaction. Furthermore, we demonstrated the cleaning capability of opened LMs on hydrophilic surfaces using a simple method. A LM was transferred onto a facile angle control platform, while a group of solid pigment particles were prepared beforehand on a hydrophilic plate to act as the pollutants. The particle coverage rate of the LM was restricted to approximately 60% and its movement was triggered randomly. Upon the initiation of rolling motion, the CMOS camera with ample depth of field was activated to observe the cleaning process of solid pollutants in real-time, which can be judged by directly observing the color change inside the LM.

Data availability

The data that support the findings of this study are available from the corresponding author upon reasonable request.

Received: 22 November 2023; Accepted: 12 April 2024;
Published online: 28 April 2024

References

1. Whitesides, G. M. The Origins and the Future of Microfluidics. *Nature* **442**, 368–373 (2006).
2. Chen, M. et al. Naked Liquid Marbles: A Robust Three-Dimensional Low-Volume Cell-Culturing System. *ACS Appl Mater. Interfaces* **11**, 9814–9823 (2019).
3. Sreejith, K. R. et al. Liquid Marbles as Biochemical Reactors for the Polymerase Chain Reaction. *Lab Chip* **19**, 3220–3227 (2019).
4. Li, L., Tian, J., Li, M. & Shen, W. Superhydrophobic Surface Supported Bioassay–an Application in Blood Typing. *Colloids Surf. B. Biointerfaces* **106**, 176–180 (2013).
5. Chen, H. et al. Continuous Directional Water Transport on the Peristome Surface of Nepenthes Alata. *Nature* **532**, 85–89 (2016).
6. Ooi, C. H. et al. Manipulation of a Floating Liquid Marble Using Dielectrophoresis. *Lab Chip* **18**, 3770–3779 (2018).
7. Hwang, H. Papadopoulos, P., Fujii, S. & Wooh, S. Driving Droplets on Liquid Repellent Surfaces *Via* Light-Driven Marangoni Propulsion. *Adv. Func. Mater*. **32**, 2111311 (2022).
8. van Assenbergh, P., Meinders, E., Geraedts, J. & Dodou, D. Nanostructure and Microstructure Fabrication: From Desired Properties to Suitable Processes. *Small* **14**, 1703401 (2018).
9. Malinowski, R., Parkin, I. P. & Volpe, G. Advances Towards Programmable Droplet Transport on Solid Surfaces and Its Applications. *Chem. Soc. Rev.* **49**, 7879–7892 (2020).
10. Huang, Z. et al. Fundamentals and Manipulation of Bare Droplets and Liquid Marbles as Open Microfluidic Platforms. *Processes* **11**, 983 (2023).
11. Aussillous, P. & Quéré, D. Liquid Marbles. *Nature* **411**, 924–927 (2001).
12. Ooi, C. H. & Nguyen, N.-T. Manipulation of Liquid Marbles. *Microfluidics Nanofluidics* **19**, 483–495 (2015).
13. Ooi, C. H. et al. Liquid Marble-Based Digital Microfluidics - Fundamentals and Applications. *Lab Chip* **21**, 1199–1216 (2021).
14. Jin, J. & Nguyen, N.-T. Manipulation Schemes and Applications of Liquid Marbles for Micro Total Analysis Systems. *Microelectron. Eng.* **197**, 87–95 (2018).
15. Saczek, J. et al. Long-Lived Liquid Marbles for Green Applications. *Adv. Func. Mater*. **31**, 2011198 (2021).
16. Aussillous, P. & Quéré, D. Properties of Liquid Marbles. *Proc. R. Soc. A: Math., Phys. Eng. Sci.* **462**, 973–999 (2006).
17. Liu, Z. et al. Larger Stabilizing Particles Make Stronger Liquid Marble. *Small* **15**, 1804549 (2019).
18. Huang, J., Wang, Z., Shi, H. & Li, X. Mechanical Robustness of Monolayer Nanoparticle-Covered Liquid Marbles. *Soft Matter* **16**, 4632–4639 (2020).
19. Ogawa, S. et al. Liquid Marbles Supported by Monodisperse Poly(Methylsilsesquioxane) Particles. *Langmuir* **30**, 9071–9075 (2014).
20. Lathia, R.; Modak, C. D. & Sen, P. Two Modes of Contact-Time Reduction in the Impact of Particle-Coated Droplets on Superhydrophobic Surfaces. *Droplet*. **2**, e89 (2023).
21. Tosun, A. & Erbil, H. Y. Evaporation Rate of Ptfe Liquid Marbles. *Appl. Surf. Sci.* **256**, 1278–1283 (2009).
22. Fullarton, C. et al. Evaporation, Lifetime, and Robustness Studies of Liquid Marbles for Collision-Based Computing. *Langmuir* **34**, 2573–2580 (2018).
23. Asaumi, Y. et al. Effect of Stabilizing Particle Size on the Structure and Properties of Liquid Marbles. *Langmuir* **36**, 13274–13284 (2020).
24. Oliveira, N. M., Reis, R. L. & Mano, J. F. The Potential of Liquid Marbles for Biomedical Applications: A Critical Review. *Adv. Healthc. Mater.* **6**, 1700192 (2017).
25. McHale, G. & Newton, M. I. Liquid Marbles: Principles and Applications. *Soft Matter*. **7**, 5473–5481 (2011).
26. Bormashenko, E. et al. Interfacial and Conductive Properties of Liquid Marbles Coated with Carbon Black. *Powder Technol.* **203**, 529–533 (2010).
27. Singha, P., Nguyen, N.-K., Zhang, J., Nguyen, N.-T. & Ooi, C. H. Oscillating Sessile Liquid Marble - a Tool to Assess Effective Surface Tension. *Colloids and Surfaces A: Physicochem. Engineering Aspects*. **627**, 127176 (2021).
28. Hamaker, H. C. The London—Van Der Waals Attraction between Spherical Particles. *Physics* **4**, 1058–1072 (1937).
29. Kralchevsky, P. A. & Nagayama, K. Capillary Interactions between Particles Bound to Interfaces, Liquid Films and Biomembranes. *Adv. Colloid Interface Sci.* **85**, 145–192 (2000).
30. Chan, D., Henry, J. Jr & White, L. The Interaction of Colloidal Particles Collected at Fluid Interfaces. *J. Colloid Interface Sci.* **79**, 410–418 (1981).
31. Bormashenko, E., Pogreb, R., Bormashenko, Y., Musin, A. & Stein, T. New Investigations on Ferrofluidics: Ferrofluidic Marbles and Magnetic-Field-Driven Drops on Superhydrophobic Surfaces. *Langmuir* **24**, 12119–12122 (2008).
32. Bormashenko, E., Bormashenko, Y. & Oleg, G. On the Nature of the Friction between Nonstick Droplets and Solid Substrates. *Langmuir* **26**, 12479–12482 (2010).
33. Macdougall, G. & Ockrent, C. Surface Energy Relations in Liquid/Solid Systems I. The Adhesion of Liquids to Solids and a New Method of Determining the Surface Tension of Liquids. *Proc. R. Soc. Lond. Ser. A. Math. Phys. Sci.* **180**, 151–173 (1942).
34. Furmidge, C. Studies at Phase Interfaces. I. The Sliding of Liquid Drops on Solid Surfaces and a Theory for Spray Retention. *J. Colloid Sci.* **17**, 309–324 (1962).
35. Briscoe, B. & Galvin, K. The Sliding of Sessile and Pendent Droplets the Critical Condition. *ColSu* **52**, 219–229 (1991).
36. Abolghasemibizaki, M., Robertson, C. J., Fergusson, C. P., McMasters, R. L. & Mohammadi, R. Rolling Viscous Drops on a Non-Wettable Surface Containing Both Micro-and Macro-Scale Roughness. *Phys. Fluids*. **30**, 023105 (2018).
37. Backholm, M., et al. Water Droplet Friction and Rolling Dynamics on Superhydrophobic Surfaces. *Commun. Mater*. **1**, 64 (2020).
38. Jin, J., Ooi, C. H., Dao, D. V. & Nguyen, N. T. Coalescence Processes of Droplets and Liquid Marbles. *Micromachines (Basel)*. **8**, 336 (2017).
39. Jin, J., Ooi, C. H., Dao, D. V. & Nguyen, N. T. Liquid Marble Coalescence Via Vertical Collision. *Soft Matter* **14**, 4160–4168 (2018).
40. Castro, J. O., Neves, B. M., Rezk, A. R., Eshtiaghi, N. & Yeo, L. Y. Continuous Production of Janus and Composite Liquid Marbles with Tunable Coverage. *ACS Appl Mater. Interfaces* **8**, 17751–17756 (2016).
41. Lekshmi, B. S. & Varanakkottu, S. N. Janus Liquid Marbles: Fabrication Techniques, Recent Developments, and Applications. *Droplet*. **20**, e44 (2023).
42. Liu, K. & Jiang, L. Bio-Inspired Self-Cleaning Surfaces. *Annu. Rev. Mater. Res.* **42**, 231–263 (2012).
43. Nishimoto, S. & Bhushan, B. Bioinspired Self-Cleaning Surfaces with Superhydrophobicity, Superoleophobicity, and Superhydrophilicity. *RSC Adv*. **3**, 671–690 (2013).
44. Blossey, R. Self-Cleaning Surfaces—Virtual Realities. *Nat. Mater.* **2**, 301–306 (2003).
45. Dalawai, S. P. et al. Recent Advances in Durability of Superhydrophobic Self-Cleaning Technology: A Critical Review. *Prog. Org. Coat.* **138**, 105381 (2020).
46. Barthlott, W. & Neinhuis, C. Purity of the Sacred Lotus, or Escape from Contamination in Biological Surfaces. *Planta* **202**, 1–8 (1997).

Acknowledgements

The authors acknowledge the financial support by National Natural Science Foundation of China (Grant number: 62204070), Basic and Applied Basic Research Foundation of Guangdong Province (Grant number:

2020A1515110901 & 2022A1515010054), and Science, Technology and Innovation Commission of Shenzhen Municipality (Grant number: GXWD20220811151610001 & RCBS20221008093249080).

Author contributions

Conceptualization, Jing Jin (J.J.) and Zheng Huang (Z.H.); Methodology, J.J., Z.H. and Yuanhao Xie (Y.X.); Investigation and validation, Z.H., Y.X. and Zheng Shen (Z.S.); Writing—original draft preparation, J.J. and Z.H.; Writing—review and editing, J.J., Bo Liu (B.L.) and Huaying Chen (H.C.); Visualization, Z.H. and Z.S.; Supervision and project administration, J.J. and H.C.; Funding acquisition, J.J.; All authors have read and agreed to the current version of the manuscript.

Competing interests

The authors declare no competing interests.

Additional information

Supplementary information The online version contains supplementary material available at https://doi.org/10.1038/s43246-024-00504-5.

Correspondence and requests for materials should be addressed to Jing Jin or Huaying Chen.

Peer review information *Communications Materials* thanks Zuankai Wang and the other, anonymous, reviewer(s) for their contribution to the peer review of this work. Primary Handling Editors: Xiaoyan Li & John Plummer.